BIOCHEMISTRY
including biophysical chemistry & molecular biology

Article

pubs.acs.org/biochemistry

Probing the Effect of Mutations of Asparagine 181 in the D1 Subunit of Photosystem II

Ravi Pokhrel,[†,§] Richard J. Debus,[*,‡] and Gary W. Brudvig[*,†]

[†]Department of Chemistry, Yale University, New Haven, Connecticut 06520-8107, United States
[‡]Department of Biochemistry, University of California, Riverside, California 92521, United States

Supporting Information

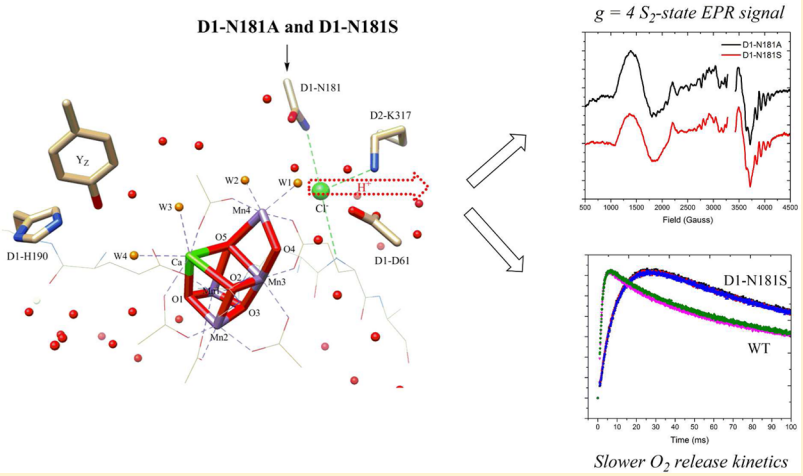

ABSTRACT: Efficient proton removal from the oxygen-evolving complex (OEC) of photosystem II (PSII) and activation of substrate water molecules are some of the key aspects optimized in the OEC for high turnover rates. The hydrogen-bonding network around the OEC is critical for efficient proton transfer and for tuning the position and pK_a values of the substrate water/hydroxo/oxo molecules. The D1-N181 residue is part of the hydrogen-bonding network on the active face of the OEC. D1-N181 is also associated with the chloride ion in the D2-K317 site and is one of the residues closest to a putative substrate water molecule bound as a terminal ligand to Mn4. We studied the effect of the D1-N181A and D1-N181S mutations on the water oxidation chemistry at the OEC. PSII core complexes isolated from the D1-N181A and D1-N181S mutants have steady-state O_2 evolution rates lower than those of wild-type PSII core complexes. Fourier transform infrared spectroscopy indicates slight perturbations of the hydrogen-bonding network in D1-N181A and D1-N181S PSII core complexes, similar to the effects of some other mutations in the same region, but to a lesser extent. Unlike in wild-type PSII core complexes, a $g = 4$ signal was observed in the S_2-state EPR spectra of D1-N181A and D1-N181S PSII core complexes in addition to the normal $g = 2$ multiline signal. The S-state cycling of D1-N181A and D1-N181S PSII core complexes was similar to that of wild-type PSII core complexes, whereas the O_2-release kinetics of D1-N181A and D1-N181S PSII core complexes were much slower than the O_2-release kinetics of wild-type PSII core complexes. On the basis of these results, we conclude that proton transfer is not compromised in the D1-N181A and D1-N181S mutants but that the O−O bond formation step is retarded in these mutants.

Photosystem II (PSII) is Nature's catalyst for light-driven water oxidation. The oxygen-evolving complex (OEC), the site for water oxidation in PSII, is a Mn_4CaO_5 core supported by amino acid residues.[1] One or more chloride ions bound near the OEC are also essential for water oxidation catalysis.[2−6] There are five redox states of the OEC, known as the S_i states (i = 0−4), relevant for light-driven water oxidation catalysis in PSII. The S_1 state is the dark-stable state of the OEC. The S_2 state of the OEC has been exhaustively characterized by various spectroscopic techniques because of the ease of trapping this state in good yield. The S_2 state of the OEC has a half-integer total spin, and electron paramagnetic resonance (EPR) spectroscopy has been very useful in characterizing the OEC in this state. In spinach PSII, two spin isomers are normally observed in the S_2 state with total ground-state spins of the Mn_4CaO_5 cluster of $S_T = {}^1/_2$ and $S_T = {}^5/_2$, respectively.[7,8] The $S_T = 1/2$ form of the OEC gives rise to a $g = 2$ multiline EPR signal, whereas the $S_T = {}^5/_2$ form of the OEC gives rise to a broad $g = 4$ EPR signal.[7,8] The equilibrium between these two forms in spinach PSII varies depending on treatments and measurement conditions.[9] In cyanobacterial PSII, the $g = 4$

Received: November 30, 2014
Revised: February 12, 2015
Published: February 13, 2015

DOI: 10.1021/bi501468h
Biochemistry 2015, 54, 1663−1672

signal has been more elusive. The $g = 4$ signal is not observed in wild-type PSII under native conditions. However, when Ca^{2+} in the OEC is substituted with Sr^{2+} in *Synechocystis* PSII or when I^- is substituted for Cl^- in *Thermosynechococcus elongatus* PSII, a $g = 4$ signal has been observed.[10,11] The $g = 4$ form of the OEC has also been observed upon mutations of some residues near the OEC.[12,13]

With the availability of high-resolution crystal structures of PSII, the identities of residues that ligate the metals in the OEC are well-resolved. Several carboxylate residues and one histidine residue serve as ligands to the Ca and Mn ions in the OEC,[14,15] and there have been numerous studies focusing on mutations of these amino acid residues.[16] Surprisingly, the majority of mutations of the direct ligands to the OEC are not detrimental to OEC assembly or to water oxidation chemistry.[17−21] However, more severe effects have been observed with mutations of amino acid residues in the proximity of the OEC that do not serve as ligands to the OEC.[13,22−28] For example, mutations of CP43-R357, D1-D61, and D2-K317 have been shown to have inefficient S-state transitions and slow O_2-release kinetics.[13,22,24−26,29] Many of these outer-sphere residues are important in the hydrogen-bonding network around the OEC or are part of the putative proton channel from the OEC to the lumen.[14,30,31]

Among the outer-sphere residues, asparagine 181 in the D1 subunit particularly stands out for two reasons. (1) X-ray crystal structures of PSII have shown that the side chain of D1-N181 has a hydrogen-bonding interaction with the chloride ion bound in the D2-K317 site,[14] and (2) D1-N181 is one of the closest residues to a putative substrate water, Mn4-bound W2 (Figure 1).[14] W2 is bound to the "dangler" Mn in the OEC,

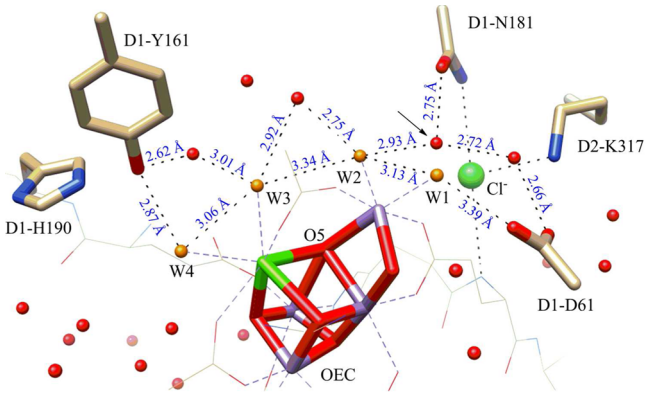

Figure 1. Position of D1-N181 relative to the Cl^- ion, D2-K317, D1-D61, the OEC, OEC-bound water molecules (W1−W4), other water molecules surrounding the OEC, D1-Y161, and D1-H190 from the 1.9 Å crystal structure.[14] The calcium ion in the OEC is colored green; the manganese ions are colored purple, and the oxo bridges are colored red. The active face of the OEC is oriented toward the top of the figure and includes the hydrogen-bonded network between water molecules and amino acid residues (blue). Distances are between two O atoms or between O and N atoms.

denoted as Mn4, as is W1 (Figure 1).[14] W1 is also directly hydrogen bonded to D1-D61, which is proposed to be one of the key residues involved in removal of protons from the OEC to the lumen; therefore, perturbations to the hydrogen-bonding network of W1 would likely impair proton removal and slow catalysis.[6,22,24,25,29,32,33] However, W2 is a putative substrate water molecule involved in O−O bond formation, and its perturbation would likely affect catalysis more severely.[1,34−36] Tuning the pK_a of W2 and positioning of the water/hydroxo/oxo form of W2 in a preferred geometry suitable for the O−O bond formation could be a critical aspect of the $S_3 \rightarrow [S_4] \rightarrow S_0$ transition. The hydrogen-bonding network around W2 also plays an important role in determining the acidity of W2 as well as the geometry of W2 in various S states. On the basis of structural information,[14] the hydrogen-bonding network near the putative substrate waters could be significantly affected by D1-N181, thereby altering the pK_a and reactivity of the substrate waters. Furthermore, D1-N181 may be important for retention of the chloride ion in its binding pocket near D2-K317. The presence of chloride ion at the D2-K317 site is thought to play a role in facilitating the transport of a proton from the OEC to the lumen.[6,13,33] Realizing the potential importance of the D1-N181 residue, which lies in the proximity of the active face of the OEC, we investigated the effects of the D1-N181A and D1-N181S mutations in PSII.

MATERIALS AND METHODS

Construction of Mutants and Purification of PSII Core Complexes. The D1-N181A and D1-N181S mutations were introduced into the *psbA-2* gene of *Synechocystis* sp. PCC 6803[37] and transformed into a host strain of *Synechocystis* that lacks all three *psbA* genes and contains a hexahistidine tag (His-tag) fused to the C-terminus of CP47.[38] Oxygen-evolving PSII core complexes were purified in 1.2 M betaine, 10% (v/v) glycerol, 50 mM MES-NaOH (pH 6.0), 20 mM $CaCl_2$, 5 mM $MgCl_2$, 50 mM histidine, 1 mM EDTA, and 0.03% (w/v) *n*-dodecyl *β*-D-maltoside as described previously[10,39,40] and stored at −196 °C (vapor phase nitrogen). To verify the integrity of the mutant cultures that were harvested for the purification of PSII core complexes, an aliquot of each culture was set aside and the sequence of the relevant portion of the *psbA-2* gene was obtained after polymerase chain reaction amplification of genomic DNA.[37] No traces of the wild-type codon were detected in any of the mutant cultures.

FTIR Spectroscopy. FTIR samples were prepared as described previously,[29,41,42] allowed to equilibrate at 0 °C in the dark in the FTIR sample compartment for 1.5 h, given six preflashes, and allowed to adapt to the dark for an additional 30 min. Sample concentrations were adjusted so that the absolute absorbance of the amide I band at 1657 cm^{-1} was 0.6−1.1. Midfrequency FTIR spectra were recorded with a Bruker Vertex 70 spectrometer (Bruker Optics, Billerica, MA) as described previously.[29] To obtain difference spectra corresponding to successive S-state transitions, the single-beam spectrum that was recorded after the *n*th flash was divided by the single-beam spectrum that was recorded immediately before the *n*th flash and the ratio was converted to units of absorption. To estimate the background noise level, the second preflash single-beam spectrum was divided by the first, and the ratio was converted to units of absorption. The sample was dark-adapted for 30 min, and then the cycle was repeated. The cycle was repeated 15 times for each sample, and the difference spectra recorded with numerous samples were averaged.

EPR Spectroscopy. EPR samples were prepared by concentrating purified PSII core complexes using Amicon Centrifugal Filter Units with a 30 kDa cutoff. EPR scans were acquired on a Bruker ELEXSYS 500 EPR spectrometer equipped with a SHQ resonator and an Oxford ESR-900 helium-flow cryostat. The S_1-state spectra were obtained in the dark using dark-adapted PSII core complexes. The S_2-state spectra were obtained after illumination of the samples in a 200

DOI: 10.1021/bi501468h
Biochemistry 2015, 54, 1663−1672

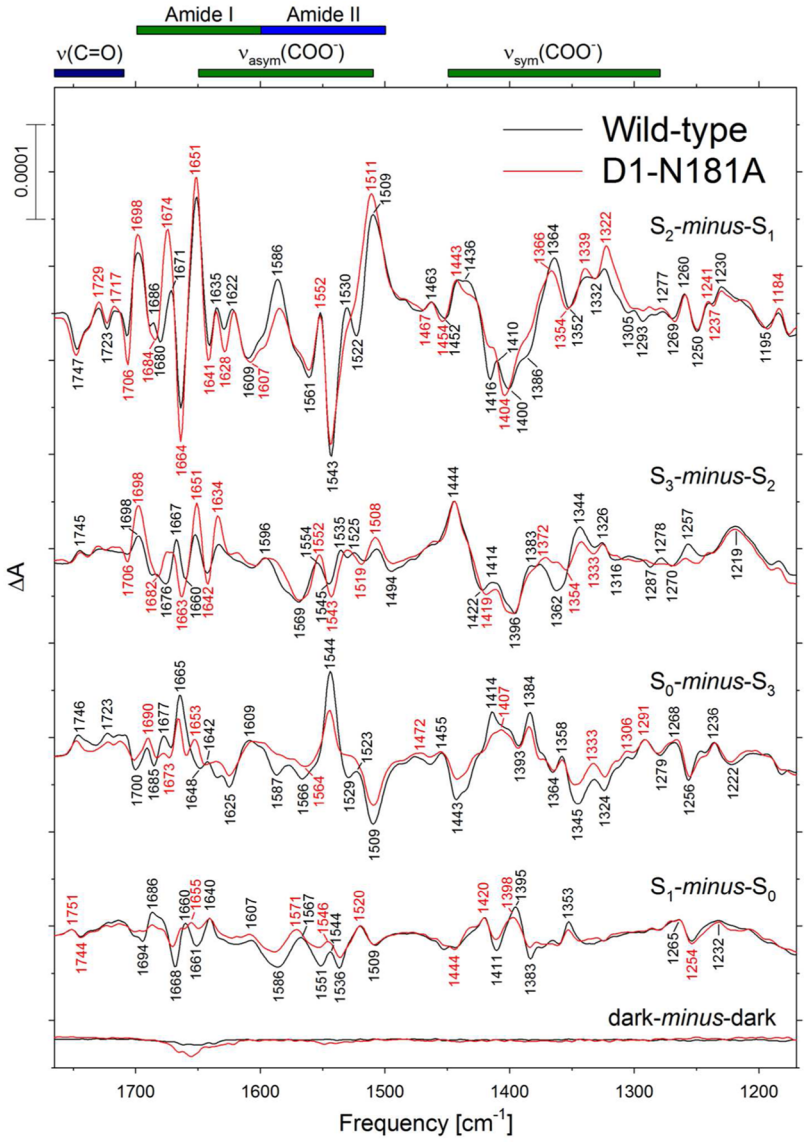

Figure 2. Comparison of the midfrequency FTIR difference spectra of wild-type (black) and D1-N181A (red) PSII core complexes in response to four successive flash illuminations applied at 0 °C. The data (plotted from 1770 to 1170 cm^{-1}) represent the averages of 14 wild-type (20100 scans for each trace) and 20 D1-N181A (30000 scans for each trace) samples. To facilitate comparisons, the mutant spectra have been multiplied vertically by factors of 1.9, 2.0, 2.0, and 1.9, respectively, after normalization to the average absolute amplitudes of the samples at the amide I peak at 1657 cm^{-1}. Dark-minus-dark control traces are included to show the noise level (bottom traces).

K dry ice/acetone bath for 5 min. EPR scans were performed at 6.5 K with the following instrumental parameters: microwave frequency, 9.39 GHz; modulation frequency, 100 kHz; modulation amplitude, 31 G; microwave power, 5 mW.

Xe Flash-Induced Oxygen Measurement. Flash-induced polarographic measurements were made using a bare platinum electrode. The electrochemical cell was comprised of a Pt disk working electrode and a Ag ring counter electrode. The Ag ring was also used as the reference electrode. Purified PSII core complexes (9 μg of Chl) were diluted to a total volume of 1 mL using a buffer containing 20% (w/v) PEG 6000, 25 mM $CaCl_2$, 50 mM NaCl, and 50 mM MES-NaOH (pH 6.5). DCBQ and K_3FeCN_6 were also added to final concentrations of 500 μM and 1 mM, respectively. PSII in PEG buffer was then added to the platinum electrode. A Teflon fitting was used in the electrode to contain the solution within the Pt electrode surface. The PSII cores were immediately centrifuged using a HS-4 swing-out rotor at 4000 rpm for 15 min in the dark. After the cores had been pelleted on the platinum disk, the Teflon fitting was removed, and an additional 1 mL of PEG buffer was added. The electrode was polarized for 10 s before data acquisition, after which time the flash sequence was initiated. For single-turnover flashes, a xenon flash lamp (#FX 249, EG&G electro-optics) triggered by a FY-712 "Lite-Pac" module (EG&G electro-optics) and a BK precision 3300 pulse generator was used in all experiments. The S-state parameters, misses and double hits, were obtained by fitting the data assuming a four-state model. Data for flash oxygen kinetics were obtained using the amperometric signal from the third-flash O_2 burst.

RESULTS

Steady-State O_2 Evolution. The light-saturated steady-state oxygen evolution activities of PSII core complexes isolated

DOI: 10.1021/bi501468h
Biochemistry 2015, 54, 1663−1672

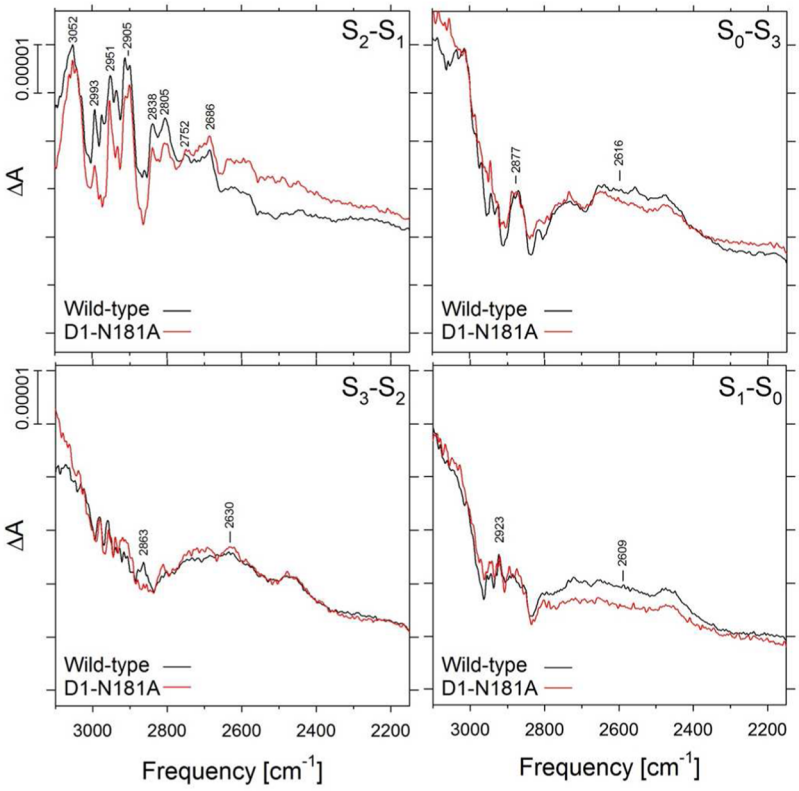

Figure 3. Comparison of the FTIR difference spectra of wild-type (black) and D1-N181A (red) PSII core complexes between 3100 and 2150 cm^{-1} in response to four successive flash illuminations applied at 0 °C. The data were collected simultaneously with that shown in Figure 2 and were normalized and expanded vertically as in Figure 2.

from the D1-N181A and D1-N181S mutants were 800−1000 μmol of O_2 (mg of Chl)$^{-1}$ h^{-1} compared to 2400−2800 μmol of O_2 (mg of Chl)$^{-1}$ h^{-1} in PSII core complexes isolated from WT.

FTIR Spectroscopy. *Midfrequency Region.* The midfrequency FTIR difference spectra induced by four successive flashes given to wild-type and D1-N181A PSII core complexes from *Synechocystis* sp. PCC 6803 are compared in Figure 2 (black and red traces, respectively). The corresponding spectra of D1-N181S PSII core complexes are shown in Figure S1 of the Supporting Information.

The spectra that are induced by the first, second, third, and fourth flashes applied to the wild-type PSII core complexes correspond predominantly to the S_2-minus-S_1, S_3-minus-S_2, S_0-minus-S_3, and S_1-minus-S_0 FTIR difference spectra, respectively.[43−46] The S_2-minus-S_1 FTIR difference spectrum of D1-N181A PSII (top red trace in Figure 2) shows small differences from the wild-type spectrum throughout the spectral region, with the most significant differences being the appearance of a large positive peak at 1674 cm^{-1}, a decreased amplitude of the 1586(+) cm^{-1} feature, the elimination of the derivative feature at 1530(+)/1522(−) cm^{-1}, the 1416 (−) cm^{-1} feature, the shoulders at 1436(+) and 1386(−) cm^{-1}, a decreased amplitude and upshift of the 1364 (+) cm^{-1} feature, and an increased amplitude of the 1322(+) cm^{-1} feature. Nearly identical differences were produced by the D1-N181S mutation (Figure S1 of the Supporting Information). The 1530(+) and 1522(−) cm^{-1} features correspond to amide II modes because they downshift appreciably after global incorporation of ^{13}C[41,47−49] or ^{15}N.[13,21,41,48,49] The 1586(+) cm^{-1} feature has been assigned to a $\nu_{asym}(COO^-)$ mode because it downshifts by 30−35 cm^{-1} after global incorporation of ^{13}C[41,47−49] but is largely insensitive to the global incorporation of ^{15}N.[13,21,41,48,49] The mutation-induced changes show that the mutation slightly alters the response of multiple carboxylate groups and the protein backbone to the positive charge that develops on the Mn_4CaO_5 cluster during the S_1-to-S_2 transition.

The D1-N181A PSII core complexes exhibited well-resolved second-, third-, and fourth-flash spectra that approximately resembled the S_3-minus-S_2, S_0-minus-S_3, and S_1-minus-S_0 FTIR difference spectra, respectively, of WT (Figure 2). The corresponding spectra of the D1-N181S PSII core complexes were nearly identical to those of D1-N181A (Figure S1 of the Supporting Information). Significant differences between the wild-type and mutant S_3-minus-S_2 spectra were the larger amplitudes of the features at 1698(+), 1663(−), 1651(+), and 1634(+) cm^{-1}, the elimination of the 1362(−) cm^{-1} feature, the near elimination of the 1257(+) cm^{-1} feature, and the substantial decrease of the magnitude of the 1344(+) cm^{-1} feature. Significant differences between the wild-type and mutant S_0-minus-S_3 spectra were the diminished amplitudes of most of the features in $\nu_{sym}(COO^-)$ and overlapping amide II/$\nu_{asym}(COO^-)$ regions. Significant differences between the wild-type and mutant S_1-minus-S_0 spectra were the near elimination of features at 1686(+), 1661(−), and 1551(−) cm^{-1} and the diminished amplitudes of the features at 1668(−), 1586(−), 1411(−), 1395(+), 1383(−), and 1353(+) cm^{-1}.

The 3100−2150 cm^{-1} Region. A broad feature centered at 3000 cm^{-1} in the S_2-minus-S_1 FTIR difference spectrum of wild-type PSII core complexes from *T. elongatus* and *Synechocystis* sp. PCC 6803 has been assigned to changes in the polarization of a highly polarized network of strong

DOI: 10.1021/bi501468h
Biochemistry 2015, 54, 1663−1672

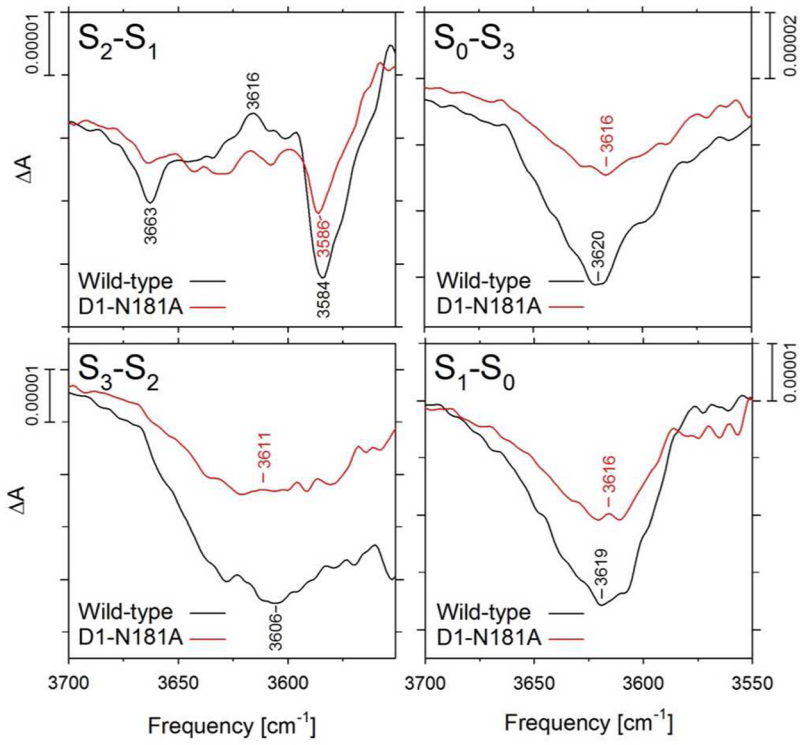

Figure 4. Comparison of the FTIR difference spectra of wild-type (black) and D1-N181A (red) PSII core complexes in the weakly hydrogen-bonded O−H stretching region in response to four successive flash illuminations applied at 0 °C. The data were collected simultaneously with that shown in Figure 2, but the mutant data were not multiplied vertically after normalization to the average absolute amplitudes of the samples at 1657 cm^{-1}. Note the different vertical scales.

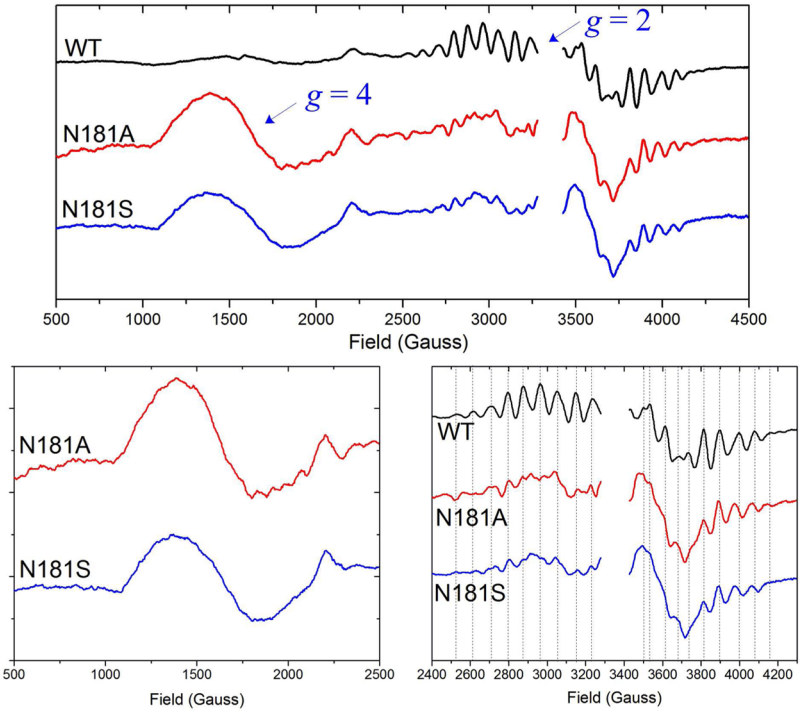

Figure 5. S_2-state illuminated-minus-dark EPR spectra of WT, D1-N181A, and D1-N181S PSII core complexes (top panel). Lower panels show expansions of the g = 4 and g = 2 regions of WT, D1-N181A, and D1-N181S PSII samples.

hydrogen bonds (known as Zundel polarizability) near the Mn_4CaO_5 cluster.[29,50,51] Similar broad features centered near 2600 cm^{-1} in the S_3-minus-S_2, S_0-minus-S_3, and S_1-minus-S_0 spectra have been assigned to the same origin.[29,50,51] In the S_2-minus-S_1 difference spectrum, a wealth of features overlays the broad feature (e.g., see Figure 3, top left panel). These features have been attributed to a mixture of C−H stretching vibrations from aliphatic groups and N−H stretching vibrations and their

DOI: 10.1021/bi501468h
Biochemistry 2015, 54, 1663−1672

Fermi resonance overtones from the imidazole group(s) of one or more histidine residues.[50,52,53] In the S_2-minus-S_1 difference spectra of D1-N181A and D1-N181S (top left panels in Figure 3 and Figure S2 of the Supporting Information, respectively), the amplitude of the broad feature may be slightly decreased, but the overlying features appear to be unchanged. The higher amplitudes of the mutant S_2-minus-S_1 spectra below 2700 cm^{-1} probably represent a shift in baseline. The broad features in the S_3-minus-S_2, S_0-minus-S_3, and S_1-minus-S_0 spectra appear to be largely unchanged by the mutations (Figure 3 and Figure S2 of the Supporting Information).

The 3700−3500 cm^{-1} Region. The O−H stretching vibrations of water molecules participating in relatively weak hydrogen bonds can be detected between 3700 and 3500 cm^{-1}.[29,50,53−56] The negative features in this region have been attributed to water molecules that are located on or near the Mn_4CaO_5 cluster and that either deprotonate or form stronger hydrogen bonds (i.e., weakly hydrogen-bonded OH groups become strongly hydrogen-bonded) during the individual S-state transitions. The features in these regions of the S_2-minus-S_1, S_3-minus-S_2, S_0-minus-S_3, and S_1-minus-S_0 spectra appear to be largely unaffected by the D1-N181A and D1-N181S mutations (Figure 4 and Figure S3 of the Supporting Information, respectively).

EPR Spectroscopy. The S_2-state EPR spectra of D1-N181A and D1-N181S have a $g = 2$ multiline signal as well as a broad $g = 4$ signal under chloride-sufficient conditions (Figure 5). The $g = 4$ signal is absent in PSII core complexes isolated from WT *Synechocystis*. The $g = 2$ multiline signals obtained from the N181A and N181S samples have slightly different peak positions from the $g = 2$ multiline signal obtained from WT (Figure 5). In the $g = 2$ multiline signals obtained for the mutants, the peaks on the low-field side are not as intense or well resolved as on the high-field side (Figure 5). Other than the differences in the EPR signals originating from the OEC, it is clear that cytochrome b_{559} is oxidized in a significant fraction of centers in D1-N181A and D1-N181S PSII (Figure S4 of the Supporting Information).

Flash-Induced O_2 Yield and O_2-Release Kinetics. PSII core complexes isolated from D1-N181A and D1-N181S have normal S-state cycling, as observed in the xenon flash-induced O_2 yield measurements (Figure S5 of the Supporting Information). The miss factor estimated by fitting the O_2 yields using a four-state Kok model is similar to that of WT (Table 1). However, the O_2-release kinetics are significantly slower in the D1-N181A and D1-N181S mutants than in WT (Figure 6). Comparison of O_2-release kinetics between D1-N181A and D1-N181S shows similar kinetics for both of the D1-N181 mutants (Figure S6 of the Supporting Information).

Table 1. Percent Misses, Double Hits, and Initial S-State Populations Calculated for D1-N181A and D1-N181S PSII Core Complexes by Fitting Flash-Dependent O_2 Yields from Figure S5 of the Supporting Information[a]

	α (% misses)	β (% double hits)	S_0 (%)	S_1 (%)	S_2 (%)	S_3 (%)
WT[b]	7.7	7.0	19.0	71.1	9.6	1.7
N181A	8.1	6.4	8.6	71.3	10.0	10.1
N181S	9.8	4.8	2.9	72.4	12.9	11.8

[a]Flashes were initiated at a frequency of 3 Hz. Fitting was done using a four-state Kok model.[57,58] [b]Data for WT were taken from ref 13.

DISCUSSION

D1-N181 is part of the hydrogen-bonding network encompassing the OEC-bound water molecules and a chloride ion (Figure 1). One or two of the OEC-bound water molecules are putative substrate water molecules.[1] The two main proposals for O−O bond formation at the OEC under debate are (1) nucleophilic attack of a Ca-bound water molecule on a Mn(IV)-$O^{\bullet}$[1,34,35] and (2) coupling of a terminal Mn(IV)-$O^{\bullet}$ and a μ-oxo group.[59−61] According to the nucleophilic attack mechanism, Ca-bound W3 and Mn-bound W2 are the most likely substrate water molecules (Figure 1). According to the terminal oxyl/bridging oxo coupling mechanism, Mn-bound W2 (or an additional water that binds in a higher S state to Mn1) and O5 μ-oxo are the most likely substrate water molecules (Figure 1). In either case, the nature of the hydrogen-bonding interactions of the substrate water molecules with the surrounding water molecules and amino acid residues will play an important role in the water oxidation catalysis at the OEC. Other than the proton-release steps, the pK_a values and geometries of the substrate water molecules may change depending on the nature of the hydrogen-bonding interactions.

The changes to the midfrequency S_2-minus-S_1 FTIR difference spectrum produced by the D1-N181A and D1-N181S mutants closely resemble those produced by the D2-K317A mutation.[13] Consequently, mutation of D1-N181 or D2-K317 in the chloride-binding pocket produces similar changes in the response of the protein to the charge that develops on the Mn_4CaO_5 cluster during the S_1-to-S_2 transition. The 1530(+)/1522(−) cm^{-1} feature that is eliminated by the D1-N181A and D1-N181S mutations is also eliminated by the D1-D61A,[29] D1-R334A,[30] D2-E312A,[31] and D2-K317A[13,27] mutations. The elimination of the same 1530(+)/1522(−) cm^{-1} feature by mutations constructed at all five residues (D1-D61, D1-N181, D1-R334, D2-E312, and D2-K317) suggests the partial disruption of a common network of hydrogen bonds that includes the $Cl^-(1)$ ion. Nevertheless, mutation of D1-N181 causes a much smaller perturbation to the overall networks of hydrogen bonds surrounding the Mn_4CaO_5 cluster and involved in transferring protons from the Mn_4CaO_5 cluster to the lumen. Unlike D1-N181A and D1-N181S, the D1-D61A, D1-R334A, D2-E312A, and D2-K317A mutations substantially decrease the efficiency of the S-state transitions as shown by the increased miss parameters in measurements of flash-induced yields of O_2. Furthermore, mutations of D1-D61, D1-R334, and D2-E312 cause substantial changes throughout the $\nu_{sym}(COO^-)$ and overlapping amide II/$\nu_{asym}(COO^-)$ regions of the S_2-minus-S_1 FTIR difference spectrum, in contrast to those of D1-N181A and D1-N181S. The modest influence of D1-N181 on the networks of hydrogen bonds that surround the Mn_4CaO_5 cluster is also shown by the modest impact of the D1-N181A and D1-N181S mutations in the 3700−3500 and 3100−2150 cm^{-1} regions of the FTIR difference spectra. In contrast to the D1-D61A[29] and D1-E333Q mutations,[56] the D1-N181A or D1-N181S mutations produce no substantial changes in the weakly hydrogen-bonding water O−H stretching regions of any of the FTIR difference spectra (Figure 4 and Figure S3 of the Supporting Information). This observation implies that the water molecules that are deprotonated or increase their hydrogen bond strengths during the individual S-state transitions do not interact with D1-N181. In contrast to the D1-D61A mutation,[29] the D1-N181A and D1-N181S mutations do not eliminate the broad feature

DOI: 10.1021/bi501468h
Biochemistry 2015, 54, 1663−1672

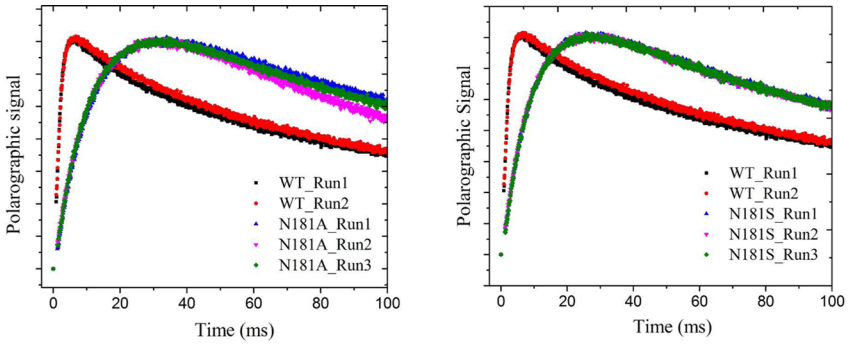

Figure 6. O_2-release kinetics of WT, D1-N181A, and D1-N181S PSII core complexes. The amperometric signals were obtained on the third flash with maximal O_2 production and are normalized to the same peak current. Three independent runs are shown for both D1-N181A and D1-N181S.

centered near 2900 cm^{-1} from the S_2-minus-S_1 FTIR difference spectrum (Figure 3 and Figure S2 of the Supporting Information). This observation implies that the highly polarizable network of hydrogen bonds whose polarizability or protonation state increases during the S_1-to-S_2 transition involves D1-D61, but not D1-N181.

As discussed earlier, two spin isomers, $S_T = {}^1/_2$ and $S_T = {}^5/_2$, of the OEC are trapped in the S_2 state. The $g = 2$ signal arises from an $S_T = {}^1/_2$ form of the OEC,[7] whereas the $g = 4$ signal arises from an $S_T = {}^5/_2$ form of the OEC.[8,62] The $g = 2$ multiline signal and the $g = 4$ signal have been extensively studied for almost three decades, mostly using PSII isolated from spinach. The $g = 2$ signal is proposed to arise when the "dangler" Mn is oxidized in the $S_1 \rightarrow S_2$ transition, whereas the $g = 4$ signal is proposed to arise when the His332-bound Mn is oxidized in the $S_1 \rightarrow S_2$ transition.[63] PSII core complexes isolated from WT cyanobacteria do not exhibit the $g = 4$ signal under native conditions.[10,64] However, under several conditions such as Sr^{2+} substitution of Ca^{2+} in the OEC,[10] I^- substitution of Cl^-,[11] and the D1-A344 and D2-K317R mutations,[12,13] the $g = 4$ signal has been observed in cyanobacterial PSII. Observation of the $g = 4$ signal in the N181A and N181S mutants gives us additional information to better understand the origin of the S_2-state $g = 4$ and $g = 2$ signals.

Density functional theory calculations suggest that in the $S_T = {}^1/_2$ form of the OEC, oxidation of the "dangler" Mn to Mn(IV) maintains the open cubane form present in the S_1 state; the His332-bound Mn remains pentacoordinate.[63,65] In the $S_T = {}^5/_2$ form of the OEC, the His332-bound Mn is oxidized to Mn(IV), triggering the O5 oxo bridge to move down to serve as a ligand to His332-bound Mn; the His332-bound Mn is hexacoordinated, while the "dangler" Mn loses the O5 ligand.[63,65] Although models for the $g = 2$ form and the $g = 4$ form of the OEC have been proposed, the mechanism of how or why the $g = 4$ form is favored over the $g = 2$ form under some conditions is not understood. With new information about the mutations that favor the $g = 4$ form over the native $g = 2$ form, we gain insight into the mechanism of origin of the $g = 4$ form of the OEC. As shown in Figure 1, the position of D1-N181 is critical in maintaining the hydrogen-bonding network encompassing W1−W4. The C═O group of D1-N181 is hydrogen bonded to the water molecule indicated with an arrow in Figure 1, which is in turn hydrogen bonded to Mn-bound W2. Mutation of D1-N181 to A or S is expected to result in a rearrangement of this hydrogen-bonding network, resulting in changes in the strength of the hydrogen bonds of Mn-bound W1 and W2 with its neighboring hydrogen-bonding partners. Such a change could be enough to favor oxidation of the His332-bound Mn over that of the "dangler" Mn in the $S_1 \rightarrow S_2$ transition in a substantial fraction of PSII reaction centers.

Several mutations to amino acid residues lying on the outer sphere of the OEC have been made, and most of these mutations lead to an increase in the miss factor during S-state transitions (Table 2). The increase in the miss factor could stem from several possibilities, including disruption of the hydrogen-bonding network as a result of the mutation that causes inefficient proton transfer. During catalysis, there are multiple proton-coupled electron-transfer steps, and any compromise in the proton transfer could lead to an increase in the miss factor. Most of the mutants that display high miss factors have also been shown to have slower O_2-release kinetics in the $S_3 \rightarrow [S_4] \rightarrow S_0$ transition (Table 2). Possibilities for the cause of slowing the O_2-release kinetics include (1) inefficient proton transfer slowing the O−O bond-forming step, which involves PCET, and (2) an inherently slow O−O bond-forming step, even in the presence of a robust proton-transfer pathway, because of an unfavorable geometry or reactivity of the substrate water molecules.

Table 2. Comparison of the Miss Factors and O_2-Release Kinetics of Mutations Constructed around the OEC

	miss factor (%)	O_2-release kinetics ($t_{1/2}$)
D1-D61N	26% vs 17% in WT[25]	15 ms vs 2.7 ms in WT[25]
	14% vs 10% in WT[22]	13.1 ms vs 1.35 ms in WT[24]
		54−56 ms vs 1.1−3.7 ms in WT[22]
D1-D61A	N/A	12 ms vs 2.7 ms in WT[25]
D1-D61E	N/A	2.7 ms vs 2.7 ms in WT[25]
CP43-R357K	46% vs 10% in WT[26]	3.2 ms vs 0.9 ms in WT[26]
D1-V185N	18% vs 14% in WT[28]	27.0 ms vs 1.2 ms in WT[28]
D1-V185T	13% vs 14% in WT[28]	1.5 ms vs 1.2 ms in WT[28]
D2-K317A	22% vs 8% in WT[13]	slow[13]
D2-K317R	18% vs 8% in WT[13]	slow[13]
D1-N181A	8% vs 8% in WT	slow
D1-N181S	10% vs 8% in WT	slow
D1-H332Q,S	10% vs 10% in WT (UV−vis method)[66]	N/A
CP43-E354Q	9% vs 9% in WT[21]	same as WT[21]

Oxygen evolution studies in the presence and absence of chloride indicate that the chloride ion is still bound in the chloride-binding pocket of D1-N181A and D1-N181S PSII core complexes (Figure S7 of the Supporting Information). In contrast, mutations of D2-Lys317 showed altered chloride binding properties.[13] These contrasting observations are

DOI: 10.1021/bi501468h
Biochemistry 2015, 54, 1663−1672

reasonable considering the ion-pair interaction between the chloride ion and D2-Lys317 is much stronger than the hydrogen-bonding interaction between D1-Asn181 and the chloride ion. Therefore, on the basis of (1) the evidence indicating the presence of the chloride ion in the D1-N181A and D1-N181S mutants, (2) the absence of substantial changes in the hydrogen-bonding network, and (3) the similarity of the miss factor to that of WT, we conclude that proton egress is not significantly affected in the D1-N181A and D1-N181S mutants. To explain the much slower O_2-release kinetics observed for the D1-N181A and D1-N181S mutants, we draw a distinction between hydrogen-bonding networks required for efficient S-state advancement and the positions and dynamics of critical water molecules required for efficient O−O bond formation. Our results indicate that the N181 mutations are distinct from other mutations around the OEC in that the proton-transfer steps are robust and unhindered in the N181 mutants. A less than optimal geometry of a substrate water/hydroxo/oxo (most probably W2 and/or W3 in Figure 1) could cause slower O−O bond formation in N181A and N181S PSII core complexes, thereby explaining the slow O_2-release kinetics caused by these mutations.

■ ASSOCIATED CONTENT

Ⓢ Supporting Information

Comparison of FTIR spectra (midfrequency, 3100−2150 cm^{-1}, and OH stretching region) of D1-N181S and WT PSII core complexes, EPR spectra of dark-adapted and 200 K illuminated samples of D1-N181A and D1-N181S PSII core complexes, flash-induced polarographic O_2 measurements of D1-N181A and D1-N181S PSII core complexes, and comparison of O_2 -release kinetics of D1-N181A and D1-N181S PSII core complexes. This material is available free of charge via the Internet at http://pubs.acs.org.

■ AUTHOR INFORMATION

Corresponding Authors

*E-mail: gary.brudvig@yale.edu. Phone: (203) 432-5202. Fax: (203) 432-6144.

*E-mail: richard.debus@ucr.edu. Phone: (951) 827-3483. Fax: (951) 827-4294.

Present Address

[§]R.P.: Department of Chemistry, University of Wisconsin—Madison, Madison, WI 06511.

Funding

This work was supported by grants from the Department of Energy, Office of Basic Energy Sciences, Division of Chemical Sciences. O_2 evolution and EPR studies were supported by Grant DE-FG02-05ER15646 (to G.W.B.). Mutant construction and FTIR studies were supported by Grant DE-FG02-10ER16191 (to R.J.D.).

Notes

The authors declare no competing financial interest.

■ ACKNOWLEDGMENTS

We are grateful to Anh P. Nguyen for maintaining the mutant and wild-type cultures of *Synechocystis* sp. PCC 6803 and for purifying the thylakoid membranes that were used for the isolation of PSII core complexes.

■ ABBREVIATIONS

DCMU, 3-(3,4-dichlorophenyl)-1,1-dimethylurea; DCBQ, 2,5-dichloro-*p*-benzoquinone; EPR, electron paramagnetic resonance; FTIR, Fourier transform infrared; OEC, oxygen-evolving complex; PSII, photosystem II.

■ REFERENCES

(1) McEvoy, J. P., and Brudvig, G. W. (2006) Water splitting chemistry of photosystem II. *Chem. Rev. 106*, 4455−4483.

(2) Bové, J. M., Bové, C., Whatley, F. R., and Arnon, D. I. (1963) Chloride requirement for oxygen evolution in photosynthesis. *Z. Naturforsch. 18b*, 683−688.

(3) Critchley, C. (1985) The role of chloride in photosystem II. *Biochim. Biophys. Acta 811*, 33−46.

(4) Homann, P. H. (1988) The chloride and calcium requirement of photosynthetic water oxidation: Effects of pH. *Biochim. Biophys. Acta 934*, 1−13.

(5) Yocum, C. F. (2008) The calcium and chloride requirements of the O_2 evolving complex. *Coord. Chem. Rev. 252*, 296−305.

(6) Pokhrel, R., McConnell, I. L., and Brudvig, G. W. (2011) Chloride regulation of enzyme turnover: Application to the role of chloride in photosystem II. *Biochemistry 50*, 2725−2734.

(7) Dismukes, G. C., and Siderer, Y. (1981) Intermediates of a polynuclear manganese center involved in photosynthetic oxidation of water. *Proc. Natl. Acad. Sci. U.S.A. 78*, 274−278.

(8) Haddy, A., Lakshmi, K. V., Brudvig, G. W., and Frank, H. A. (2004) Q-band EPR of the S_2 state of photosystem II confirms an S = 5/2 origin of the X-band g = 4.1 signal. *Biophys. J. 87*, 2885−2896.

(9) Pokhrel, R., and Brudvig, G. W. (2014) Oxygen-evolving complex of photosystem II: Correlating structure with spectroscopy. *Phys. Chem. Chem. Phys. 16*, 11812−11821.

(10) Strickler, M. A., Walker, L. M., Hillier, W., and Debus, R. J. (2005) Evidence from biosynthetically incorporated strontium and FTIR difference spectroscopy that the C-terminus of the D1 polypeptide of photosystem II does not ligate calcium. *Biochemistry 44*, 8571−8577.

(11) Boussac, A., Ishida, N., Sugiura, M., and Rappaport, F. (2012) Probing the role of chloride in Photosystem II from *Thermosynechococcus elongatus* by exchanging chloride for iodide. *Biochim. Biophys. Acta 1817*, 802−810.

(12) Mizusawa, N., Yamanari, T., Kimura, Y., Ishii, A., Nakazawa, S., and Ono, T.-A. (2004) Changes in the functional and structural properties of the Mn cluster induced by replacing the side group of the C-terminus of the D1 protein of photosystem II. *Biochemistry 43*, 14644−14652.

(13) Pokhrel, R., Service, R. J., Debus, R. J., and Brudvig, G. W. (2013) Mutation of lysine 317 in the D2 subunit of photosystem II alters chloride binding and proton transport. *Biochemistry 52*, 4758−4773.

(14) Umena, Y., Kawakami, K., Shen, J.-R., and Kamiya, N. (2011) Crystal structure of oxygen-evolving photosystem II at a resolution of 1.9 Å. *Nature 473*, 55−60.

(15) Suga, M., Akita, F., Hirata, K., Ueno, G., Murakami, H., Nakajima, Y., Shimizu, T., Yamashita, K., Yamamoto, M., Ago, H., and Shen, J.-R. (2015) Native structure of photosystem II at 1.95 Å resolution viewed by femtosecond X-ray pulses. *Nature 517*, 99−103.

(16) Debus, R. J. (2008) Protein ligation of the photosynthetic oxygen-evolving center. *Coord. Chem. Rev. 252*, 244−258.

(17) Chu, H.-A., Debus, R. J., and Babcock, G. T. (2001) D1-Asp170 is structurally coupled to the oxygen evolving complex in photosystem II as revealed by light-induced Fourier transform infrared difference spectroscopy. *Biochemistry 40*, 2312−2316.

(18) Strickler, M. A., Walker, L. M., Hillier, W., Britt, R. D., and Debus, R. J. (2007) No evidence from FTIR difference spectroscopy that aspartate-342 of the D1 polypeptide ligates a Mn ion that undergoes oxidation during the S_0 to S_1, S_1 to S_2, or S_2 to S_3 transitions in photosystem II. *Biochemistry 46*, 3151−3160.

DOI: 10.1021/bi501468h
Biochemistry 2015, 54, 1663−1672

(19) Strickler, M. A., Hillier, W., and Debus, R. J. (2006) No evidence from FTIR difference spectroscopy that glutamate-189 of the D1 polypeptide ligates a Mn ion that undergoes oxidation during the S_0 to S_1, S_1 to S_2, or S_2 to S_3 transitions in photosystem II. *Biochemistry 45*, 8801−8811.
(20) Debus, R. J., Strickler, M. A., Walker, L. M., and Hillier, W. (2005) No evidence from FTIR difference spectroscopy that aspartate-170 of the D1 polypeptide ligates a manganese ion that undergoes oxidation during the S_0 to S_1, S_1 to S_2, or S_2 to S_3 transitions in photosystem II. *Biochemistry 44*, 1367−1374.
(21) Service, R. J., Yano, J., McConnell, I., Hwang, H.-J., Niks, D., Hille, R., Wydrzynski, T., Burnap, R. L., Hillier, W., and Debus, R. J. (2011) Participation of Glutamate-354 of the CP43 Polypeptide in the Ligation of Manganese and the Binding of Substrate Water in Photosystem II. *Biochemistry 50*, 63−81.
(22) Dilbeck, P. L., Hwang, H. J., Zaharieva, I., Gerencser, L., Dau, H., and Burnap, R. L. (2012) The D1-D61N mutation in *Synechocystis sp.* PCC 6803 allows the observation of pH-sensitive intermediates in the formation and release of O_2 from photosystem II. *Biochemistry 51*, 1079−1091.
(23) Singh, S., Debus, R. J., Wydrzynski, T., and Hillier, W. (2008) Investigation of substrate water interactions at the high-affinity Mn site in the photosystem II oxygen-evolving complex. *Philos. Trans. R. Soc., B 363*, 1229−1234.
(24) Clausen, J., Debus, R. J., and Junge, W. (2004) Time-resolved oxygen production by PSII: Chasing chemical intermediates. *Biochim. Biophys. Acta 1655*, 184−194.
(25) Hundelt, M., Hays, A.-M. A., Debus, R. J., and Junge, W. (1998) Oxygenic photosystem II: The mutation D1-D61N in *Synechocystis* sp. PCC 6803 retards S-state transitions without affecting electron transfer from Y_Z to P_{680}^+. *Biochemistry 37*, 14450−14456.
(26) Hwang, H. J., Dilbeck, P., Debus, R. J., and Burnap, R. L. (2007) Mutation of arginine 357 of the CP43 protein of photosystem II severely impairs the catalytic S-state cycle of the H_2O oxidation complex. *Biochemistry 46*, 11987−11997.
(27) Suzuki, H., Yu, J., Kobayashi, T., Nakanishi, H., Nixon, P. J., and Noguchi, T. (2013) Functional roles of D2-Lys317 and the interacting chloride ion in the water oxidation reaction of photosystem II as revealed by Fourier transform infrared analysis. *Biochemistry 52*, 4748−4757.
(28) Dilbeck, P. L., Bao, H., Neveu, C. L., and Burnap, R. L. (2013) Perturbing the Water Cavity Surrounding the Manganese Cluster by Mutating the Residue D1-Valine 185 Has a Strong Effect on the Water Oxidation Mechanism of Photosystem II. *Biochemistry 52*, 6824−6833.
(29) Debus, R. J. (2014) Evidence from FTIR difference spectroscopy that D1-Asp61 influences the water reactions of the oxygen-evolving Mn_4CaO_5 cluster of photosystem II. *Biochemistry 53*, 2941−2955.
(30) Service, R. J., Hillier, W., and Debus, R. J. (2014) Network of hydrogen bonds near the oxygen-evolving Mn_4CaO_5 cluster of photosystem II probed with FTIR difference spectroscopy. *Biochemistry 53*, 1001−1017.
(31) Service, R. J., Hillier, W., and Debus, R. J. (2010) Evidence from FTIR difference spectroscopy of an extensive network of hydrogen bonds near the oxygen-evolving Mn_4Ca cluster of photosystem II involving D1-Glu65, D2-Glu312, and D1-Glu329. *Biochemistry 49*, 6655−6669.
(32) Ferreira, K. N., Iverson, T. M., Maghlaoui, K., Barber, J., and Iwata, S. (2004) Architecture of the Photosynthetic Oxygen-Evolving Center. *Science 303*, 1831−1838.
(33) Rivalta, I., Amin, M., Luber, S., Vassiliev, S., Pokhrel, R., Umena, Y., Kawakami, K., Shen, J.-R., Kamiya, N., Bruce, D., Brudvig, G. W., Gunner, M. R., and Batista, V. S. (2011) Structural-functional role of chloride in photosystem II. *Biochemistry 50*, 6312−6315.
(34) Vrettos, J. S., Limburg, J., and Brudvig, G. W. (2001) Mechanism of photosynthetic water oxidation: Combining biophysical studies of photosystem II with inorganic model chemistry. *Biochim. Biophys. Acta 1503*, 229−245.
(35) Pecoraro, V. L., Baldwin, M. J., Caudle, M. T., Hsieh, W.-Y., and Law, N. A. (1998) A proposal for water oxidation in photosystem II. *Pure Appl. Chem. 70*, 925−929.
(36) Sproviero, E. M., Gascon, J. A., McEvoy, J. P., Brudvig, G. W., and Batista, V. S. (2008) Quantum mechanics/molecular mechanics study of the catalytic cycle of water splitting in photosystem II. *J. Am. Chem. Soc. 130*, 3428−3442.
(37) Chu, H.-A., Nguyen, A. P., and Debus, R. J. (1994) Site-directed photosystem II mutants with perturbed oxygen-evolving properties. 1. Instability or inefficient assembly of the manganese cluster in vivo. *Biochemistry 33*, 6137−6149.
(38) Debus, R. J., Campbell, K. A., Gregor, W., Li, Z.-L., Burnap, R. L., and Britt, R. D. (2001) Does histidine 332 of the D1 polypeptide ligate the manganese cluster in photosystem II? An electron spin echo envelope modulation study. *Biochemistry 40*, 3690−3699.
(39) Tang, X.-S., and Diner, B. A. (1994) Biochemical and spectroscopic characterization of a new oxygen-evolving photosystem II core complex from the cyanobacterium *Synechocystis* PCC 6803. *Biochemistry 33*, 4594−4603.
(40) Lakshmi, K. V., Reifler, M., Chisholm, D., Wang, J., Diner, B., and Brudvig, G. (2002) Correlation of the cytochrome c_2 content of cyanobacterial photosystem II with the EPR properties of the oxygen-evolving complex. *Photosynth. Res. 72*, 175−189.
(41) Yamanari, T., Kimura, Y., Mizusawa, N., Ishii, A., and Ono, T.-a. (2004) Mid- to low-frequency Fourier transform infrared spectra of S-state cycle for photosynthetic water oxidation in *Synechocystis* sp. PCC 6803. *Biochemistry 43*, 7479−7490.
(42) Noguchi, T., and Sugiura, M. (2002) Flash-induced FTIR difference spectra of the water oxidizing complex in moderately hydrated photosystem II core films: Effect of hydration extent on S-state transitions. *Biochemistry 41*, 2322−2330.
(43) Noguchi, T. (2008) Fourier transform infrared analysis of the photosynthetic oxygen-evolving center. *Coord. Chem. Rev. 252*, 336−346.
(44) Noguchi, T. (2013) Monitoring the reactions of photosynthetic water oxidation using infrared spectroscopy. *Biomed. Spectrosc. Imaging 2*, 115−128.
(45) Noguchi, T. (2015) Fourier transform infrared difference and time-resolved infrared detection of the electron and proton transfer dynamics in photosynthetic water oxidation. *Biochim. Biophys. Acta 1847*, 35−45.
(46) Debus, R. J. (2015) FTIR studies of metal ligands, networks of hydrogen bonds, and water molecules near the active site Mn_4CaO_5 cluster in Photosystem II. *Biochim. Biophys. Acta 1847*, 19−34.
(47) Noguchi, T., Sugiura, M., and Inoue, Y. (1999) In *Fourier Transform Spectroscopy: Twelfth International Conference* (Koichi, I., Tasumi, M., Eds.) pp 459−460, Waseda University Press, Tokyo.
(48) Noguchi, T., and Sugiura, M. (2003) Analysis of flash-induced FTIR difference spectra of the S-state cycle in the photosynthetic water-oxidizing complex by uniform ^{15}N and ^{13}C isotope labeling. *Biochemistry 42*, 6035−6042.
(49) Kimura, Y., Mizusawa, N., Ishii, A., Yamanari, T., and Ono, T.-a. (2003) Changes of low-frequency vibrational modes induced by universal ^{15}N- and ^{13}C-isotope labeling in S_2/S_1 FTIR difference spectrum of oxygen-evolving complex. *Biochemistry 42*, 13170−13177.
(50) Noguchi, T., and Sugiura, M. (2002) FTIR detection of water reactions during the flash-induced S-state cycle of the photosynthetic water-oxidizing complex. *Biochemistry 41*, 15706−15712.
(51) Noguchi, T., Suzuki, H., Tsuno, M., Sugiura, M., and Kato, C. (2012) Time-resolved infrared detection of the proton and protein dynamics during photosynthetic oxygen evolution. *Biochemistry 51*, 3205−3214.
(52) Noguchi, T., Inoue, Y., and Tang, X.-S. (1999) Structure of a histidine ligand in the photosynthetic oxygen-evolving complex as studied by light-induced Fourier transform infrared difference spectroscopy. *Biochemistry 38*, 10187−10195.
(53) Noguchi, T., and Sugiura, M. (2000) Structure of an active water molecule in the water-oxidizing complex of photosystem II as studied by FTIR spectroscopy. *Biochemistry 39*, 10943−10949.

DOI: 10.1021/bi501468h
Biochemistry 2015, 54, 1663−1672

(54) Noguchi, T. (2008) FTIR detection of water reactions in the oxygen-evolving centre of photosystem II. *Philos. Trans. R. Soc., B 363*, 1189−1195.
(55) Hou, L.-H., Wu, C.-M., Huang, H.-H., and Chu, H.-A. (2011) Effects of ammonia on the structure of the oxygen-evolving complex in photosystem II as revealed by light-induced FTIR difference spectroscopy. *Biochemistry 50*, 9248−9254.
(56) Service, R. J., Yano, J., Dilbeck, P. L., Burnap, R. L., Hillier, W., and Debus, R. J. (2013) Participation of glutamate-333 of the D1 polypeptide in the ligation of the Mn_4CaO_5 cluster in photosystem II. *Biochemistry 52*, 8452−8464.
(57) Forbush, B., Kok, B., and McGloin, M. P. (1971) Cooperation of charges in photosynthetic oxygen evolution. II. Damping of flash yield oscillation, deactivation. *Photochem. Photobiol. 14*, 307−321.
(58) Kok, B., Forbush, B., and McGloin, M. (1970) Cooperation of charges in photosynthetic oxygen evolution. I. A linear four step mechanism. *Photochem. Photobiol. 11*, 457−475.
(59) Messinger, J. (2004) Evaluation of different mechanistic proposals for water oxidation in photosynthesis on the basis of Mn_4O_xCa structures for the catalytic site and spectroscopic data. *Phys. Chem. Chem. Phys. 6*, 4764−4771.
(60) Siegbahn, P. E. M. (2009) Structures and energetics for O_2 formation in photosystem II. *Acc. Chem. Res. 42*, 1871−1880.
(61) Cox, N., Retegan, M., Neese, F., Pantazis, D. A., Boussac, A., and Lubitz, W. (2014) Electronic structure of the oxygen-evolving complex in photosystem II prior to O-O bond formation. *Science 345*, 804−808.
(62) Haddy, A., Dunham, W. R., Sands, R. H., and Aasa, R. (1992) Multifrequency EPR investigations into the origin of the S_2-state signal at g = 4 of the oxygen-evolving complex. *Biochim. Biophys. Acta 1099*, 25−34.
(63) Pantazis, D. A., Ames, W., Cox, N., Lubitz, W., and Neese, F. (2012) Two interconvertible structures that explain the spectroscopic properties of the oxygen-evolving complex of Photosystem II in the S_2 state. *Angew. Chem., Int. Ed. 51*, 9935−9940.
(64) Boussac, A., Sugiura, M., Inoue, Y., and Rutherford, A. W. (2000) EPR study of the oxygen evolving complex in His-tagged photosystem II from the cyanobacterium *Synechococcus elongatus*. *Biochemistry 39*, 13788−13799.
(65) Krewald, V., Neese, F., and Pantazis, D. A. (2013) On the magnetic and spectroscopic properties of high-valent Mn_3CaO_4 cubanes as structural units of natural and artificial water-oxidizing catalysts. *J. Am. Chem. Soc. 135*, 5726−5739.
(66) Sugiura, M., Rappaport, F., Hillier, W., Dorlet, P., Ohno, Y., Hayashi, H., and Boussac, A. (2009) Evidence that D1-His332 in photosystem II from *Thermosynechococcus elongatus* interacts with the S_3-state and not with the S_2-state. *Biochemistry 48*, 7856−7866.

DOI: 10.1021/bi501468h
Biochemistry 2015, 54, 1663−1672